Optimal Trajectory Planning For Material Handling of Compliant Sheet Metal Parts

Huifang Li
General Motors Corporation
Warren, MI 48092
email: huifang.li@gm.com

Dariusz Ceglarek
Department of Industrial Engineering
University of Wisconsin-Madison
Madison, WI 57306
e-mail: darek@engr.wisc.edu

One of the most critical issues in the material handling of compliant objects is excessive part deformation. The deformation of compliant sheet metal parts during the handling process can significantly impact both part dimensional quality and production rate. Increasing production rate while maintaining part quality requires an optimal design of the part transfer trajectory. This paper describes a new methodology of time-optimal trajectory planning for compliant parts by discretizing the part transfer path into N segments that have equal horizontal distance and by approximating the trajectory as having piecewise constant acceleration that can only change its value at the end of each segment. The contribution of the methodology is that part deformation determined by transfer velocity and acceleration is considered as a nonlinear constraint, which is obtained from FEA simulation and model fitting. Part permanent deformation, trajectory smoothness, and static obstacle avoidance are also considered. The methodology is validated by simulations at different motion conditions and obstacle configurations. This paper addresses the lack of current design guidelines for material handing development and simultaneously provides a mathematical tool to significantly enhance the production efficiency in manufacturing of compliant sheet metal parts. [DOI: 10.1115/1.1463035]

1 Introduction

Material handling of compliant objects/parts is of increasing concern in manufacturing automation. The handling of compliant sheet metal parts in the stamping process has recently received increased attention [1–5] due to its significant impact on product quality and productivity. Compliant sheet metal parts are widely used in various industries, such as aerospace, automobile, and appliance industries. One of the most critical issues in material handling of sheet metal parts is part deformation during the handling process. Excessive deformation may cause permanent (plastic) part deformation due to material yield. Part elastic deformation also affects part/subassembly dimensional quality mainly in the following ways:

(a) Nesting error—error of positioning/dropping parts into the die (installed in the stamping press). Part elastic deformations may cause part positional variation in a die, which can further cause mis-stamped parts in stamping press line (a stamping line for large automotive parts usually has 4-5 presses/dies). These small deviations of the part in each die accumulate and can, at times, eventually cause, very large dimensional variation of the final part that can further lead to scrap or production line downtime. This large variation can be on the level of 4-5 mm or even larger (as measured by 6-sigma).

(b) Part distortion during die contact. At the end of the material handling process, parts are usually dropped into the die. If excessive elastic deformations exist relative to the die contour, the contact force of the part with the die could be so unevenly distributed that the part could be permanently damaged.

(c) Part-obstacle interference. Part elastic deformation during transfer increases uncertainty in planning a part transfer trajectory. This may, in effect, cause unexpected interference of the part with the surrounding environment and therefore, damaging the part.

All these factors will result in deterioration of product quality and/or decrease of production rate by increase of down time. Material handling was identified as one of the top five causes of part dimensional variation [1]. It has also been observed that material in a stamping facility spends over ninety percent of its time waiting to be processed [6].

Figure 1 illustrates part transfer between two adjacent press stations in a sheet metal stamping line. When the first press ram goes up, the material handling system picks up the stamped part and transfers it forward to the next press station, then unloads the part there before the press ram runs down for next forming operation. Although, sometimes parts need to be rotated/tilted for easy placement to the next press station, in most cases parts cannot be rotated due to limitation of the handling system. During this transfer process, the sheet metal part can be deformed. The rectangular area enclosing the deformed part forms the envelope of the part deflection.

There exist direct relations among transfer path, transfer velocity and part deformation. Small transfer velocity causes cycle time increase, but also results in small part deformation. On the other hand, large transfer velocity reduces cycle time, but increases part deformation considerably, which has negative impact on part quality (in a stamping line, part transfer time is usually larger than the time of part stamping operations. Thus, production cycle time is significantly influenced by part transfer time). Currently in stamping manufacturing process, part transfer path and transfer velocity are set up based on a trial-and-error method, which is not only time-consuming, but the results are not optimal. In addition, no scientific prediction for further improvement can be provided using the 'trial and error' method. In order to achieve high efficiency of sheet metal part transfer and at the same time to avoid part damage or the deterioration of part dimensional quality (as measured by dimensional variation), it is important to develop systematic methodology to find optimal part transfer trajectory.

The problem of trajectory planning of compliant parts can be described in two ways: (1) minimize transfer time for given part deformation specification; and (2) minimize part deformation for given transfer time. In this paper, we assume the allowed maximum part deformation range is given based on requirement for the part dimensional variation. The focus is to develop an optimal trajectory along which part deformation is allowed within the required specification with minimal transfer time.

There exist a wealth of research in the area of robotics and

Contributed by the Design Automation Committee for publication in the JOURNAL OF MECHANICAL DESIGN. Manuscript received October 2000. Associate Editor: G. M. Fadel.

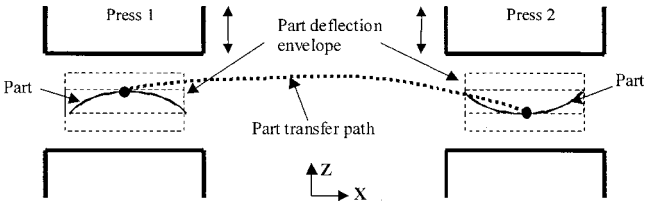

Fig. 1 Schematic plot of compliant part transfer in a stamping line

computer vision addressing path planning and motion planning problems [7,8]. The research, summarized in [9,10], is focused on designing paths and motion profiles to avoid static or dynamic environmental obstacles (collision detection and avoidance principles) by considering speed, acceleration and path curvature bounds [7,8]. During the 90's in robotics research, a new instance of the motion planning problem, sometimes called nonholonomic motion planning, had been considered: planning motions in the presence of kinematic constraints (and always amidst obstacles). It turned out to be a difficult task even in the absence of obstacles. Today there is no general algorithm to plan motions for such a system which can guarantee reaching a given goal. The only existing results are based on the approximate methods or exact methods for special classes of systems [11]. Few studies take into account moving obstacles and dynamic constraints simultaneously [12,13]. In this aspect, Fraichard [13] first explicitly presented the concept of *state-time space*, i.e. the state space of the robot augmented by time dimension. It stems from two concepts which have been used before: (1) *configuration-time space* [7]—dealing with moving obstacles; and (2) *state space*, i.e. the space of the configuration parameters and their derivatives—dealing with dynamic constraints. The trajectory planning in dynamic workspaces is then to simply find a curve in state-time space, i.e. a continuous sequence of state-times between the current state of the robot and a goal state. Smoothness of the trajectory was considered most recently by Constantinescu and Croft [14]. In their research, the third derivative of the path parameter with respect to time is a control input to reduce highly jerky motion.

Motivated by the obvious relationship between task execution time and productivity, minimum-time control problem has become one of the most extensively studied robot trajectory planning problems. Based on the path constraint, the minimum-time control problem can be divided into two categories: (1) point-to-point motion [15,16] and (2) path following motion [17,18]. The work of Kahn and Roth [15] is considered to be the first in the field of time-optimal control. The approaches that allow to solve this problem can be categorized into two groups: the standard optimal control theoretical approaches based on Pontryagin's minimum principle [19–21], and the nonstandard approximation approaches such as nonlinear parameter optimization methods [18] and dynamic programming methods [22,23].

However, the aforementioned research only deals with planning of rigid or point objects (parts). The results are not directly applicable for material handling of compliant part motion planning because part deflection should be considered as a constraint that depends on the motion direction and velocity. For example, when moving compliant parts (objects), the time-minimum path is not always the distance-minimum path between the starting point and target point due to part deflection and obstacle avoidance of the motion. The problem of motion planning for compliant objects/parts is different from, and usually more complex than that of motion planning for rigid objects.

Only a handful of studies were found on handling flexible objects. However, they addressed problems different from the focus in this paper. Zheng and Chen [24] researched trajectory planning for two robot manipulators to deform flexible beams. The flexible part-beam is intentionally deformed to certain designed shape by the control of the end effector motion trajectories. Lamiraux and Kavraki [25] designed a path planner for elastic plates based on principle of probabilistic roadmaps. They used Bezier curves to represent part deformation and assumed that the plate is manipulated in accordance with a set of user-defined grasping constraints that specify the position and orientation of two opposite edges. This model permits the computation of the shape of the plate with respect to the grasping constraints by minimizing the energy function of the deformation of the plate. They addressed problem of obstacle avoidance, however, time factor is not considered in their study. In an effort to reduce vibration during part transfer, Chen and Zheng [26] studied the effect of inertia forces caused by beam motion on the vibration of the beam in various motion patterns. They demonstrated that by proper motion planning, it is possible to reduce the vibration of the beam when it is moved. Yuen and Bone [27] proposed a method to reduce vibration based on control of the orientation of the part relative to its path. In these two studies, the purpose is only to reduce vibration and the transfer path is predefined. Transfer time is not optimized.

In this paper, we research time-minimum trajectory planning for compliant parts. The developed methodology finds the path geometry and motion parameters simultaneously. In addition to the velocity and acceleration bounds from the transfer system capability, we consider part deformation, material yield, as well as smoothness bounds of the transfer path. Furthermore, static obstacles are also included in this study. Part ''tilting'' motion during handling is not considered in this paper due to its relatively low applicability in stamping industry. This paper presents the first effort in time-optimal trajectory planning with consideration of compliant part physical properties.

This paper is organized as follows: Section 2 presents the formulation of the trajectory planning problem with focus on generation of the part deformation and material yield constraints. Section 3 explains the approach to the solution of the trajectory planning problem. Section 4 presents computer simulations for various system configurations including multi-obstacle avoidance, various part deflection specifications, and various path smoothness requirements. Finally, Section 5 summarizes and draws conclusions.

2 Trajectory Planning Model Formulation

In this section, first, the general model development is presented for trajectory planning. Then, the procedure for formulation of the material yield and part deflection constraints is developed. Next, we use an example to illustrate the developed procedure which consists of Finite Element Analysis (FEA) of part deformation and von Mises stresses during the transfer process, and data processing/analysis of the maximum part deflection and maximum von Mises stress relative to part transfer acceleration.

2.1 Problem Formulation. The trajectory planning model for the compliant sheet metal parts can be stated as follows:

1. ***Objective function***

$$\min: J = \int_0^{t_f} 1 dt \tag{1}$$

where t_f stands for the final time of transfer motion.

2 ***Boundary conditions***

$$\vec{q}(0) = \vec{q}_0$$
$$\vec{q}(t_f) = \vec{q}_f \tag{2}$$

where $\vec{q} \in R^2$ is a variable consisting of part position and transfer velocity. $\vec{q}_0$ and $\vec{q}_f$ are given initial and final values of variable $\vec{q}$.

3 ***Constraints***

(i) the path geometric constraints (to avoid static obstacle),

$$g = g(s) \tag{3}$$

where s stands for path, g(s) represents the paths that satisfy the static obstacle avoidance condition. This constraint requires the optimal path to be one of the feasible paths that can pass through obstacles presented in the environment without damaging the transferred part (an explicit example of Eq. (3) is presented as Eq. (18)).

(ii) the path smoothness constraint,

$$|\dot{\vec{a}}| \leqslant \dot{\vec{a}}_{\max} \tag{4}$$

where $\vec{a}$ is motion acceleration, $\dot{\vec{a}}$ stands for the acceleration changing rate. This constraint means that in order to meet the requirement of path smoothness, the transfer acceleration changing rate can not exceed certain value $\dot{\vec{a}}_{\max}$. The acceleration changing rate is also called as jerk.

(iii) the material handling system constraint,

$$\dot{\vec{q}}_{\min} \leqslant \dot{\vec{q}} \leqslant \dot{\vec{q}}_{\max} \tag{5}$$

where $\dot{\vec{q}}$ consists of motion velocity and acceleration. $\dot{\vec{q}}_{\min}$ and $\dot{\vec{q}}_{\max}$ represent the material handling system transfer capability.

(iv) the material yield constraint,

$$f_1(\vec{a}, \vec{v}) \leqslant \sigma_y \tag{6}$$

where $\vec{v}$ is motion velocity, σ_y is the material yield stress, f_1 is a function of $\vec{a}$ and $\vec{v}$ (see Eq. (12) for an example of an explicit expression). This constraint is to limit the maximum stress to be less than the yield stress. We use the maximum von Mises stress of the part as a criterion to compare with the yield stress. The relation of the maximum von Mises stress to the part transfer acceleration usually is nonlinear. It can be obtained from FEA analysis and statistical data processing. The details can be found in Sections 2.2 and 2.3.

(v) part deflection constraint,

$$f_2(\vec{a}, \vec{v}) \leqslant Def_{\max} \tag{7}$$

where f_2 is a function of $\vec{a}$ and $\vec{v}$, $Def_{\max}$ denotes the allowed maximum part deflection. The maximum deformation of every point on the part in any instant should not exceed this value. As presented in Section 1, part deformation constraint is based on the assumption that the allowable maximum part deformation range is given. This constraint usually is also nonlinear and can be obtained by FEA analysis and data processing presented in the next section.

2.2 Development of material yield and part deflection constraints. The nonlinear constraints expressed by Eq. (6) and (7) can be obtained by FEA analysis and data processing. FEA analysis is needed to find the relationship between the maximum stress of deformed part and the transfer acceleration due to the generally complex part shape and deformation caused by the acceleration. When von Mises stress is used as an index to compare with the yield stress, it is an equivalent stress and does not linearly relate to either horizontal acceleration or vertical acceleration, nor can it be expressed accurately through analytical relationship. Due to the same reason, FEA is needed to find the relationship between the part deflection and transfer acceleration. Even for a simple-shaped part, e.g. a rectangular blank, only at limited end effector locations the aforementioned relation can have analytical solutions [28,29].

To find the relationship between the maximum von Mises stress and the acceleration as well as between the maximum part deflection with the acceleration, a FEA-based three-step procedure is developed: (1) design a total number of *m* FEA simulations with acceleration as variable; (2) conduct each of the *m* FEA simulations; (3) perform nonlinear regression analysis to model the obtained data.

Step 1. Design of FEA simulations. In order to obtain applicable accuracy in the design of FEA simulations, the selected acceleration values should span the range in industrial applications. The total number of simulations *m* is determined by the acceleration levels of a_x and a_z. A full design can be used when the industrial application range is not large. When the industrial application range is large, considering the computational cost of the FEA analysis, the Design of Experiments (DOE) technique can be used in order to use smaller number of FEA simulations to obtain scientific results. The description of DOE techniques can be found in many statistical books such as the one authored by Wu and Hamada [30].

Step 2. FEA simulations. In the FEA analysis, we assume the number of end effectors and the end effector locations are given. The locations can take the optimal locations found from the end effector location optimization methodology [4]. They are fixed during the entire transfer process. The most commonly used end effectors in material handling for stamping process are finger/shovels and vacuum suction cups. Their characteristics can be represented by a point model [4] or a dexterous spring model [5], respectively. In the FEA model, the boundary condition is related to the end effector model and the end effector locations. The loading is acceleration-caused inertia force.

Step 3. Data processing. Each FEA analysis outputs the maximum von Mises stress and the maximum part deflection value under given acceleration. Combining all the maximum von Mises stress and the maximum part deflection value corresponding to the given acceleration and performing nonlinear regressional data fitting by using nonlinear polynomial functions, we can obtain the relationship of the maximum von Mises stress with acceleration and the maximum part deflection with acceleration:

$$\begin{aligned} M_{\max} &= f_1(\vec{a}) \\ D_{\max} &= f_2(\vec{a}) \end{aligned} \tag{8}$$

Enforcing

$$\begin{aligned} M_{\max} &\leqslant \sigma_y \\ D_{\max} &\leqslant Def_{\max} \end{aligned} \tag{9}$$

we thus obtain the constraints expressed in Eqs. (6) and (7). It can be seen that in Eq. (8), the velocity $\vec{v}$ is not a variable. This is because in this paper, we did not consider the wind resistance which is related to velocity. However, the developed methodology is equally applicable when wind resistance is considered.

2.3 An Example. In order to illustrate the procedure to generate the material yield and part deflection constraints, we use a flat rectangular sheet metal blank as an example. The blank size is 120 mm$\times$800 mm with thickness of 0.6 mm. The elastic modulus E is 2.07×10^5 MPa and Poisson's ratio is $\nu=0.3$. The center of the part is set as the origin of the coordinate system. The end effector locations are placed at ($\pm$270mm, $\pm$200mm) (Fig. 2). In Fig. 2, E1 through E4 represent the four end effectors used for part handling.

In design of the FEA simulations, the selected acceleration values span the range in industrial applications. In this example, since part is symmetric and the end effector locations are also symmetric about the YOZ plane, the magnitude of the von Mises stress and the maximum part deflection will be the same for accelerations in positive or negative signs. Therefore, the design variable levels can be reduced by using only values with the same sign. The applied acceleration values for this example are listed in Table 1. Each FEA simulation is conducted with a combination of a_x and a_z values. As listed in Table 1, a_x value has six levels and a_z has nine levels. Thus a full design with a total of fifty-four ($m=54$) FEA simulations is conducted.

In each FEA analysis, since the blank geometry and deformation are symmetric about XOZ plane in which the path planning is to take place, we use half of the blank to model the whole part (1200×400) in order to reduce the calculation cost (Fig. 3). The rectangular part is meshed using S4R5 shell elements. For most meshes, the size is 20 mm$\times$20 mm. Since the stress concentration takes place near the end effector holding positions, to obtain more accurate value of the maximum stress, the meshes in the area

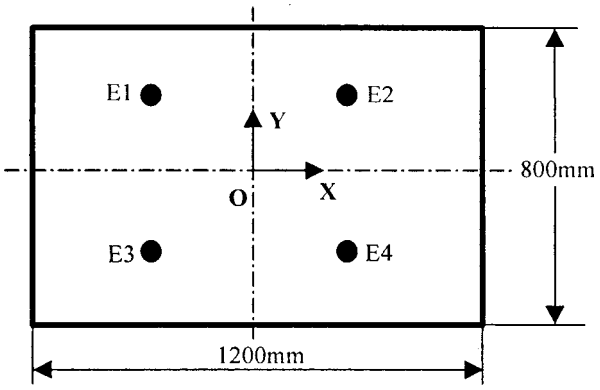

Fig. 2 An example of a sheet metal blank with end effector layout

around the end effector holding positions have higher density than that in the rest area. Rigid point model is used to model end effectors.

One example of part deformation from FEA analysis is given in Fig. 4. In the figure, the applied loading is: $a_x = -10$ m/s^2, $a_z = 10$ m/s^2.

Each FEA analysis outputs the maximum von Mises stress and the maximum part deflection value under the given combination of a_x and a_z values. After all FEA analysis is conducted, polynomial function is used to fit the maximum von Mises stress and the maximum part deflection data as a function of acceleration variable. In our simulation, a_x is negative and a_z is positive. The sign only indicates the direction of the applied loading. For this example, since the influence of acceleration on von Mises stress and part deflection range does not depend on the sign of acceleration, therefore, the generalized relationship in the entire variable domain can be obtained:

The relationship of the maximum von Mises stress with acceleration,

$$M_{\max} = -0.0625a_z^2 + 0.0443|a_x a_z| + 9.4111|a_z| + 0.5604|a_x| \tag{10}$$

Table 1 Applied acceleration values in the FEA simulation

$a_x(m/s^2)$ \ $a_z(m/s^2)$	2.5	5.0	7.5	10.0	12.5	15.0	17.5	20.0	25.0
0	1	7	13	19	25	31	37	43	49
-5.0	2	8	14	20	26	32	38	44	50
-10.0	3	9	15	21	27	33	39	45	51
-15.0	4	10	16	22	28	34	40	46	52
-20.0	5	11	17	23	29	35	41	47	53
-25.0	6	12	18	24	30	36	42	48	54

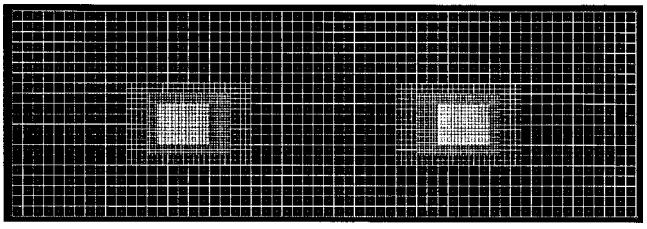

Fig. 3 Geometry mesh of the sample blank

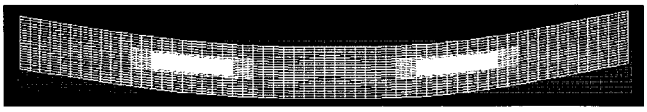

Fig. 4 An example of displaced mesh with $a_x = -10$ m/s^2, $a_z = 10$ m/s^2

The relationship of the maximum part deflection with the acceleration,

$$D_{\max} = -0.0677a_z^2 + 0.0808a_x^2 + 0.1988|a_x a_z| + 5.6105|a_z| - 1.7467|a_x| + 2.995 \tag{11}$$

The order of the model is determined by examining the R-squared value.

Therefore, the material yield stress constraint and the maximum part deflection constraint can be obtained as follows:

$$-0.0625a_z^2 + 0.0443|a_x a_z| + 9.4111|a_z| + 0.5604|a_x| \leq \sigma_y \tag{12}$$

$$-0.0677a_z^2 + 0.0808a_x^2 + 0.1988|a_x a_z| + 5.6105|a_z| - 1.7467|a_x| + 2.995 \leq Def_{\max} \tag{13}$$

Figure 5 and Fig. 6 show the FEA simulation data, the data predicted by the model fitted from the FEA simulation data, as well as the difference between these two set of data.

For a non-symmetric part, accelerations in both signs should be used in design of FEA simulations. After the FEA simulations, model fitting should be conducted using the entire set of data obtained.

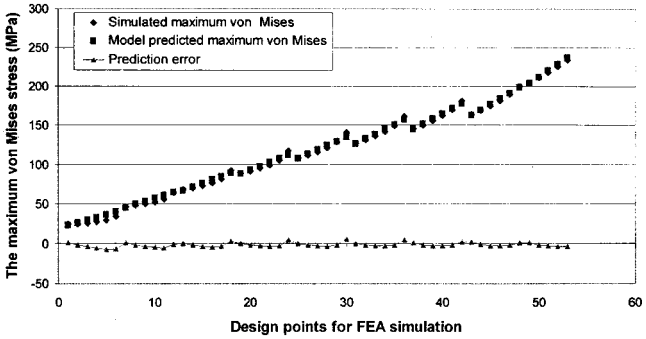

Fig. 5 Data fitting for the maximum von Mises stress

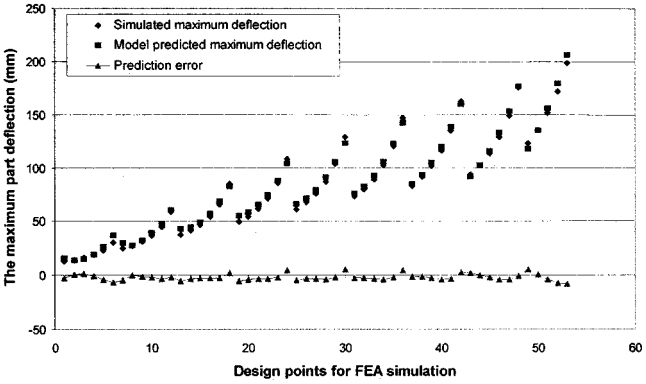

Fig. 6 Data fitting for the maximum part deflection

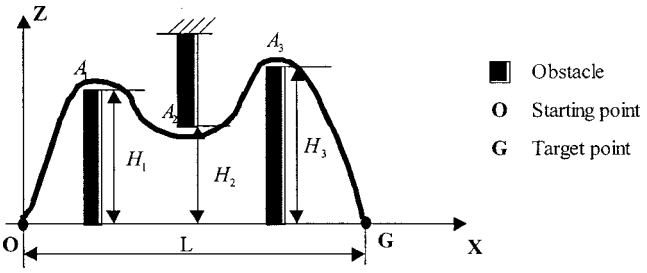

Fig. 7 Diagram of system configuration

3 Solutions to the Trajectory Planning Problem

One approach to the trajectory planning problem is state space method based on control theory. Pontryagin's maximum principle can be used to solve the problem [20]. However, for only a few limited cases the analytical solution can be obtained. Therefore, we select discrete system approach by first discretizing the continuous functions into discrete functions, then using commercial nonlinear software package to solve it.

The part transfer system configuration can be shown in Fig. 7. In Fig. 7, point O stands for the starting point for the trajectory planning and G stands for the target point. Line OG is chosen to be the horizontal axis (*x*-axis) of the coordinate system. OZ is the vertical axis. The sheet metal part is to be transferred in the XOZ plane. Points A_1, A_2, A_3 represent boundaries of three static obstacles among $A_1, A_2, \cdots, A_n$, where n is the number of obstacles. In this paper, the physical shape of the obstacles is not considered except the position in Z direction. The position of A_1, A_2, A_3 in Z direction is H_1, H_2, H_3, respectively. Part must be transferred above obstacle point A_1 and A_3, and below obstacle point A_2. The distance between points O and G is L. In the discretization, the distance of OG is divided into N segments with increment equal to h. The transfer trajectory is approximated as having piecewise constant acceleration that can only change its value at the end of each segment. The trajectory planning problem is then transformed into the following formulation:

$$\text{Min } J = \sum_{i=1}^{N} t_i \tag{14}$$

Subject to the constraints:

(1) Equation of motion

$$\begin{cases} v_x(i+1) = v_x(i) + a_x(i) \cdot t(i+1) \\ v_z(i+1) = v_z(i) + a_z(i) \cdot t(i+1) \\ x(i+1) = x(i) + v_x(i) \cdot t(i+1) + 1/2 \cdot a_x(i) \cdot [t(i+1)]^2 \\ z(i+1) = z(i) + v_z(i) \cdot t(i+1) + 1/2 \cdot a_z(i) \cdot [t(i+1)]^2 \end{cases} \tag{15}$$

where i=0,1,2, . . . $N-1$, and N is the total number of segments between points O and G.

(2) Boundary conditions,

$$x(0)=0, \quad y(0)=0; \quad v_x(0)=0, \quad v_z(0)=0 \tag{16}$$

$$x(N)=L, \quad y(N)=0; \quad v_x(N)=0, \quad v_z(N)=0 \tag{17}$$

(3) Path geometric constraints,

$$h=L/N, \quad z_{A_1} \geqslant H_1, \quad z_{A_2} \leqslant H_2, \quad z_{A_3} \geqslant H_3 \tag{18}$$

(4) Trajectory smoothness constraint,

$$|a_{i+1} - a_i|_{x,z} \leqslant \Delta a_{\max} \tag{19}$$

(5) Material handling system constraint,

$$\begin{aligned} a_{x_{\min}} \leqslant a_x(i) \leqslant a_{x_{\max}} \\ a_{z_{\min}} \leqslant a_z(i) \leqslant a_{z_{\max}} \end{aligned} \tag{20}$$

(6) Material yield constraint,

$$f_1[\vec{v}(i), \vec{a}(i)] \leqslant \sigma_y, \quad \mathbf{i}=0,1,\ldots,N \tag{21}$$

(7) Part deformation constraint,

$$f_2[\vec{v}(i), \vec{a}(i)] \leqslant Def_{\max}, \quad \mathrm{i}=0,1,\ldots,N \tag{22}$$

where $a_{x_{\min}}$, $a_{x_{\max}}$, $a_{z_{\min}}$, $a_{z_{\max}}$, and $\Delta a_{\max}$, are given constants which depend on the requirements of the material handling system used. The meanings of these constants have been presented in Section 2.1.

In case of three-dimensional obstacles, we may choose the highest or the lowest point (maximum or minimum Z value) in each section of the part, which is parallel to the YOZ plane, to form a profile of the obstacle in the XOZ plane. Whether the highest or the lowest point is to be chosen depends on which portion of the obstacle will block the part transfer. Then this profile can be discretized into p separate one-dimensional objects as $A_1, A_2, A_3, \ldots, A_p$. The height of these objects can be denoted as $H_1, H_2, H_3, \ldots, H_p$. Then the path geometric constraints can be formulated accordingly.

To solve the above problem, the software package AMPL (A Modeling Language for Mathematical Programming) [31] is used. The optimization objective function and constraint functions are programmed into the model file and initial conditions and other parameters are input in the data file. A large-scale nonlinear optimization solver "LANCELOT" [32,33] is selected as the optimization engine. The kernel algorithm of LANCELOT is an adaptation of a trust region method to the general nonlinear optimization problem subject to simple bounds. The method is extended to accommodate general constraints by using an augmented Lagrangian formulation and the bounds are handled directly and explicitly via projections that are easy to compute.

In the context to unconstrained optimization, the basic idea of trust region methods is to approximately minimize a model of the objective function in a local neighborhood (called the *trust* region) centered at the current point. The objective function is modeled about the current point $x^k \in \Re^n$, where k is the iteration count and x is the n-vector of variables. To minimize the model in the trust region, a step s^k is taken at iteration k to arrive at the point $x^k + s^k$. The function is evaluated at this point to determine how well the model predicted the actual change in the objective function. If good descent is obtained, the approximate minimizer is accepted as the next iterate ($x^{k+1} \leftarrow x^k + s^k$) and the trust region is expanded. If moderate descent is obtained, the trust region size remains unchanged, but the step is accepted. Otherwise, no new point is accepted and the trust region is contracted.

The extension to the problem with simple bounds is essentially to find the minimum along the projected gradient path within the trust region, where the projection is with respect to the bounds within the trust region.

The extension to handle equality constraints is carried out by means of an augmented Lagrangian function:

$$\Phi(a, \lambda, \mu) = J(a) + \sum_{i=1}^{m} \lambda_i c_i(a) + \frac{1}{2\mu} \sum_{i=1}^{m} c_i(a)^2 \tag{23}$$

Here $J(a)$ is the objective function, a represents the variables of the optimization, $c_i(a)$ is an equality constraint with λ_i being the corresponding Lagrangian multiplier and μ the penalty parameter used to dynamically weight feasibility. Using the earlier algorithm Φ is minimized subject to the explicit bounds. Inequality constraints are converted to equality constraints by first introducing slack variables if necessary and then formulating the augmented Lagrangian as before. This approach can be summarized as follows:

(1) Test for convergence using the two following conditions. *Sufficient stationarity*—the projected gradient of the augmented

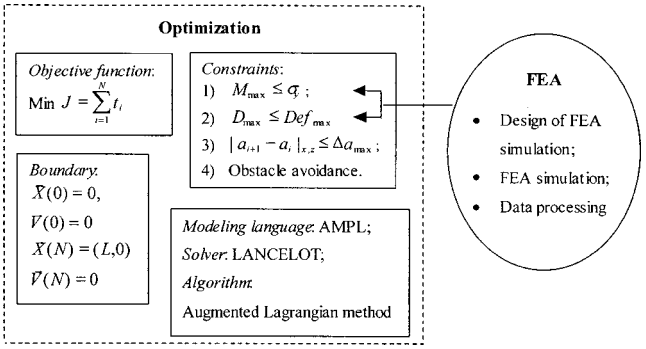

Fig. 8 Outline of the optimization methodology

Lagrangian with respect to simple bounds is sufficiently small, and *sufficient feasibility*—the norm of the constraint violations is sufficiently small.

(2) Use the simple bound algorithm to find an approximate stationary point (minimizer) of Φ subject to simple bounds.

(3) If sufficiently feasible, update the multipliers λ_i and decrease the tolerances for stationarity and feasibility.

(4) Otherwise, give more weight to feasibility (decrease μ) and reset tolerances for stationarity and feasibility.

Under suitable conditions, convergence to a first-order stationary point for nonlinear programming problem can be attained. Details about the solver can be found in Conn et al. [34].

The methodology for time-optimal trajectory planning can be summarized in Fig. 8. The FEA-based three-step procedure generates the constraints for yield stress and the maximum part deflection (Section 2.2). Then the AMPL package is used to conduct the optimization.

4 Optimization Simulation

To verify the feasibility and validity of the developed methodology, computer simulations are conducted under various conditions of obstacle layouts, maximum part deflection specifications, and trajectory smoothness requirements. In the simulation, the sheet metal part is the same as given in Section 2.3 (Fig. 3). The discretized problem formulation is as described in Section 3. The horizontal distance of transfer is L = 2.5m. The number of distance segments in the optimization is set as N = 10. The itemized description is as follows:

(1) The equations of motion is as in Eq. (15) with N = 10;

(2) The boundary condition is as in Eqs. (16) and (17), with L = 2.5;

(3) The material handling system constraint is $|a_x| \leqslant 20$ m/s^2, $|a_z| \leqslant 10$ m/s^2;

(4) The material yield constraint is given in Eq. (12);

The maximum part deflection constraint is given in Eq. (13). The simulation will be conducted for various values of $Def_{\max}$.

Since the material yield constraint and maximum part deflection constraint are the only nonlinear constraints in the optimization, it is helpful to gain an insight on the shape of these two constraints. Firstly, the part deflection constraint is analyzed. Two examples of the constraint area are shown in Fig. 9.

It can be seen from the figure that (1) with the increase of the maximum part deflection specification, the feasible area of the constraint increases, which is in accordance with the common knowledge; (2) when the maximum part deflection specification is 40mm, the constraint area is convex; when the maximum part deflection specification is 90mm, the constraint area is not convex. From simulations with various part deflection specifications, it is found that the constraint area shape changes continuously. The convexity of the area switches at a critical value of $D_{\max}$ which can be found by solving $d^2a_z/da_x^2 = 0$. For the part used in the simulation, the critical value of $D_{\max}$ is found to be 72.68mm.

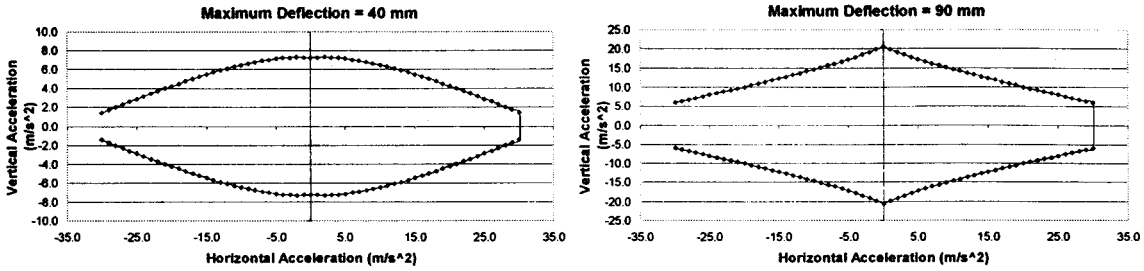

Fig. 9 Examples of part deflection constraint

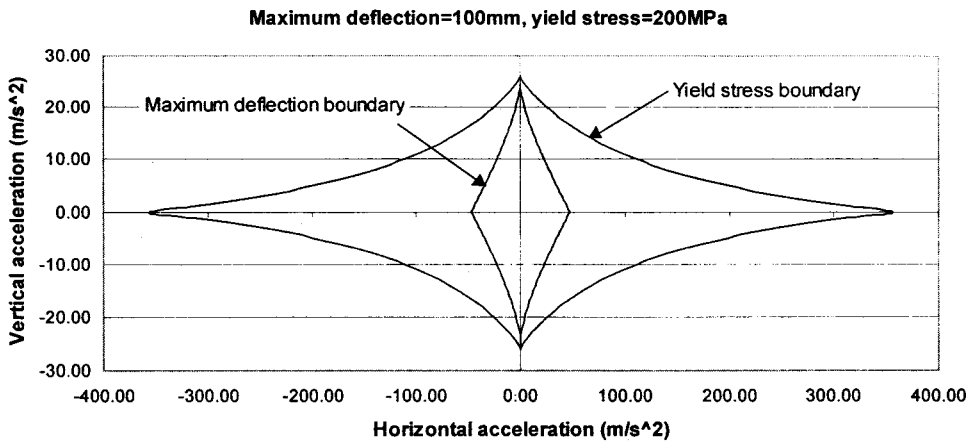

Fig. 10 Yield boundary and the maximum deflection boundary

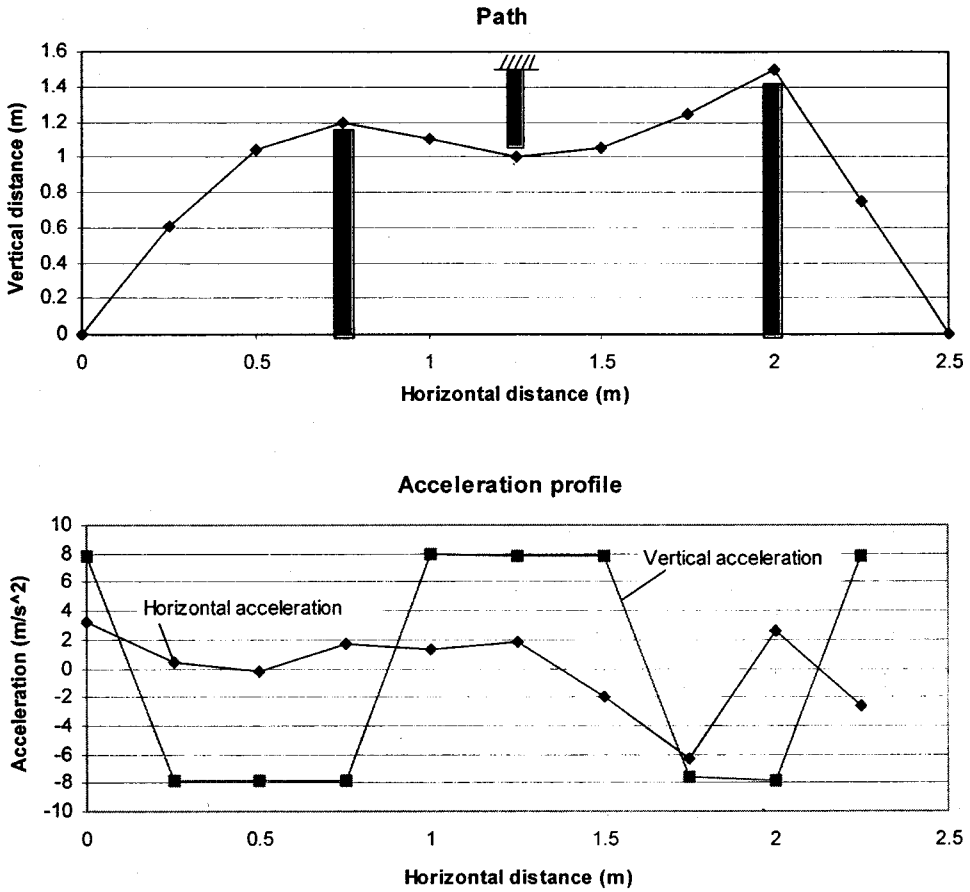

Fig. 11 Examples of trajectory planning among three obstacles

Secondly, the relationship of the material yield constraint and the maximum part deflection constraint is analyzed. Figure 10 shows the yield stress boundary (outer boundary) and the maximum deflection boundary with the maximum deflection range as 100mm (inner boundary). It can be seen that the yield stress constraint is not active in the presence of relatively small part deflection specification.

In this paper, we only present the simulations with the maximum part deflection range smaller than 100mm. Thus, the material yield stress constraint is not active. However, the developed methodology works equally well when the material yield stress constraint is active.

Three types of simulations were conducted: (1) simulation of ability to find time-optimal trajectory among static obstacles; (2) simulation under various part deflection specifications; and (3) simulation under various path smoothness requirements.

4.1 Simulation of Obstacle Avoidance. Simulations using developed optimization methodology were conducted with various number of static obstacles present in different configurations in the transfer. Figure 11 shows an example of the optimization result when three obstacles are present with configuration as in Fig. 7.

In this example, A_1 is located at (0.75m, 1.2m), A_2 is at (1.25m, 1.0m), and A_3 is at (2.0m, 1.5m). The optimal path and optimal acceleration are shown in the figure. The optimal transfer time is 2.49 seconds. The accuracy of the optimization can be improved by increasing the number of segment N. In this case, $N=10$.

It can be seen that the developed methodology can find time-optimal trajectory among complex-configured static obstacles in the surrounding environment. The capability of obstacle avoidance of the developed methodology makes it superior to the currently used tryout method in the industry. When more and complex-configured obstacles are present, it is very difficult by tryout to find a feasible trajectory for part transfer, and it is almost impossible by tryout to obtain an optimal trajectory.

4.2 Simulation Under Various Part Deflection Specifications. For this group of simulations, it is assumed that there is only one obstacle represented by point A_2 in the configuration shown in Fig. 7. Obstacles A_1 and A_3 are not present. Part must be transferred above the obstacle. Point A_2 is located at (1.25m, 1m). The optimal time and path length under various part deflection specifications are listed in Table 2. The optimal paths with different deflection specifications are shown in Fig. 12.

From the optimization results listed in Table 2, it can be seen that when the allowed maximum deflection is relatively small (below 60mm), with the increase of the allowed maximum deflection, the transfer time decreases. However, the geometric length of the optimal path is not necessarily reduced. It can also be seen that when the allowed maximum deflection reaches 60mm, the optimal transfer time remains at 1.26 seconds without further decrease. Detailed analysis reveals this is due to the simple boundary from the acceleration (material handling system capability) in the vertical direction, which can be seen from Fig. 13. In Fig. 13, the

Table 2 Optimization results under various part deflection specifications

The maximum deflection (mm)	30	40	50	60	80
Total time (seconds)	1.67	1.47	1.33	1.26	1.26
Path length (m)	3.207	3.233	3.235	3.229	3.209

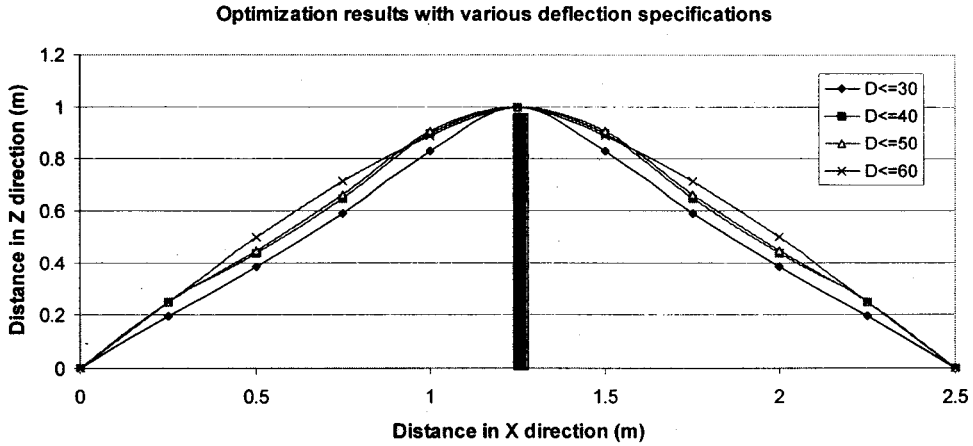

Fig. 12 Optimal paths with different maximum deflection specifications

vertical acceleration reached the maximum boundary value for each motion segment. Thus, there is no further room to reduce the transfer time.

An example of velocity plot and acceleration plot for the case when the maximum deflection is 30mm is given in Fig. 14. In this case, the deflection constraint is active in each segment.

4.3 Simulation Under Various Path Smoothness Requirements. In practice, trajectory smoothness has a positive effect on the transfer performance. The trajectory smoothness is closely related to the vibration of transferred part. Among factors impacting part vibration magnitude, change in acceleration rate is one of the most critical ones. We introduce a new variable named "jerk" which is defined as the acceleration difference between successive segments. By controlling this variable, we can control the changes in acceleration speed in the successive segments, and therefore, control part vibration. In this paper, the trajectory smoothness is represented by the value of the jerk. It is understood that when the jerk value is small, the trajectory smoothness is high.

The same example as in Section 4.2 is used with one obstacle A_2. The maximum part deflection range is defined as 60mm. The optimization was conducted with various jerk values and the results are listed in Table 3. The horizontal acceleration has much less influence on part deformation magnitude, thus the jerk constraint is only applied in vertical direction that plays a key role.

It can be seen that the smoothness has negative impact on motion time. With increased requirement of smoothness, the jerk value is decreased, the optimal time is increased, and the maximum acceleration provided by the material handling system ($10m/s^2$) is less utilized. This can be helpful for design of material handling systems by considering both the smoothness requirement and its full capability.

The optimal paths for these simulations are shown in Fig. 15. It can be seen that with smaller jerk limit, although the trajectory smoothness increases, the geometric path deviates further from the straight line formed by connecting the starting point (or the target point) with the point above the obstacle. This is a very interesting finding. In practice, it means that in order to reduce part vibration such that part quality and material handling system performance are maintained, the part transfer path should deviate from the straight line transfer, what in effect elongates the overall path length.

4.4 Summary of the Simulation and Discussions. Simulations indicate that the developed methodology of trajectory planning for compliant sheet metal parts is effective when multiple static obstacles are present in the environment and the obstacles are located in different complex configurations (e.g., formed in convex shape, concave shape, or combination of segments of convex and concave shapes).

Simulations also indicate that the developed methodology can handle various material handling system conditions. The methodology is effective when the maximum part deflection range is an active constraint, the material handling system transfer capability is an active constraint, or trajectory smoothness is an active constraint. The simulations show that below the material handling

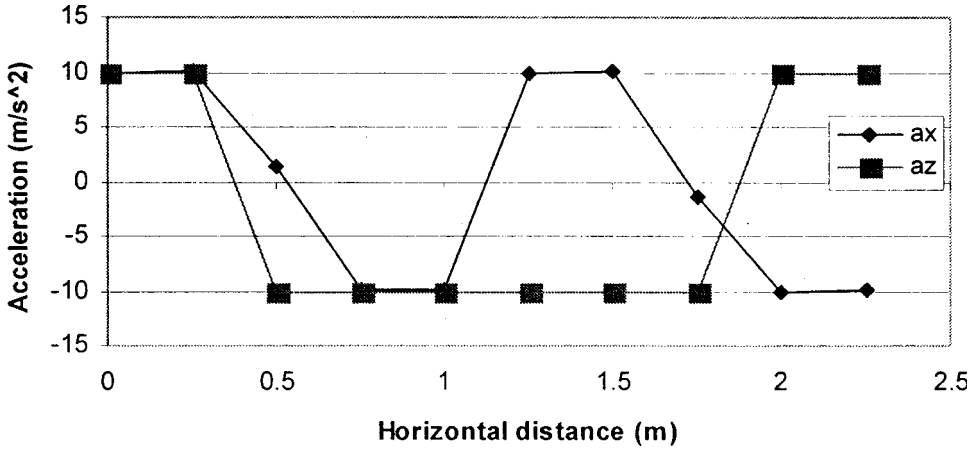

Fig. 13 Acceleration profile when the maximum deflection is 60 mm

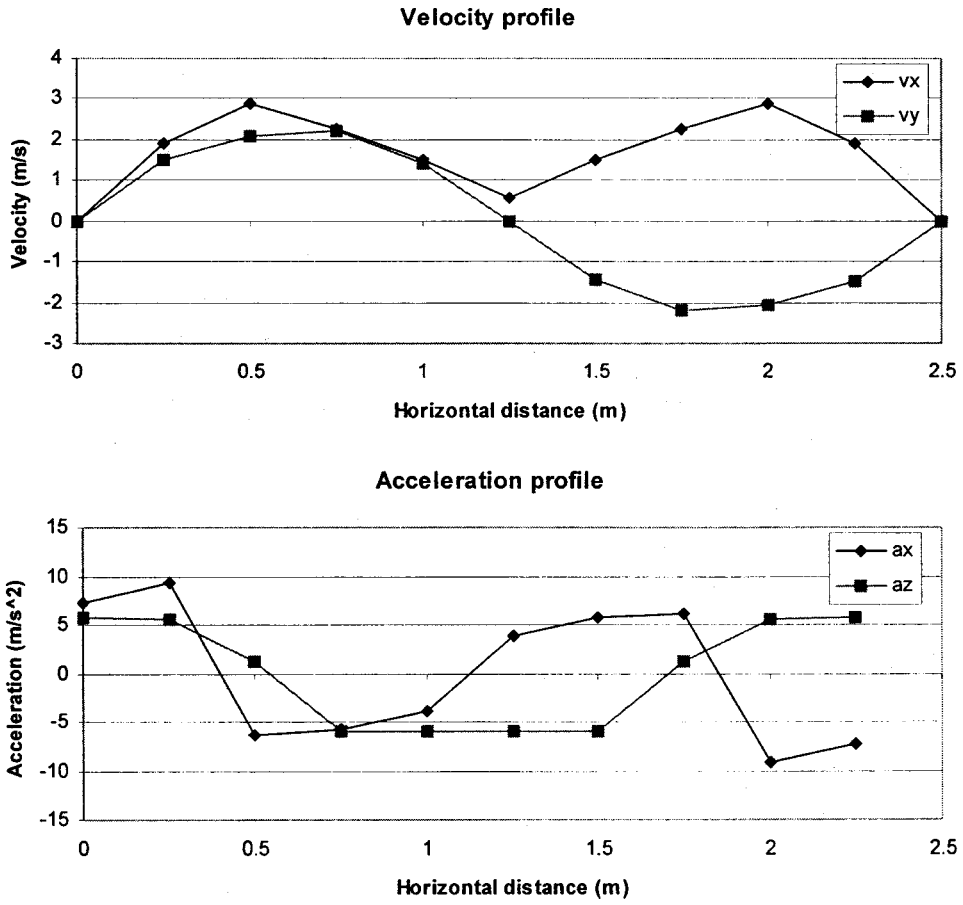

Fig. 14 Optimal trajectory when the maximum deflection is 30 mm

system capability, with the increase of part deflection specification, the optimal transfer time is reduced. However, the length of the geometric path is not necessarily shortened. The simulations show that when trajectory smoothness is increased by reduction of the jerk limit, the geometrical deviation of the transfer path from the straight line path increases.

Table 3 Comparison of optimization for various jerk values

Jerk(m/s^3)	20	5	3.5	2
Optimal time (sec)	1.2649	1.3118	1.5548	2.0418
Max. part deflection (mm)	62.995	62.906	40.483	21.954

5 Conclusions

Material handling of compliant objects is of frequent concern in manufacturing automation. One of the most critical issues in material handling of sheet metal parts is part deformation during handling, which may cause quality deterioration of part or de-

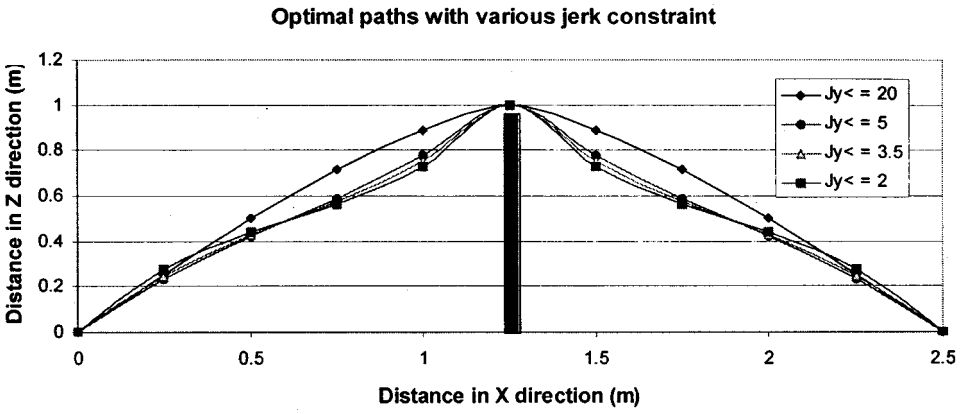

Fig. 15 Optimal trajectory with jerk constraint

crease of production rate. Reducing transfer time while maintaining part quality requires optimization of the part transfer trajectory.

This paper presents the methodology for minimum-time trajectory planning for material handling of compliant sheet metal parts by discretizing the part transfer path into N segments that have equal horizontal distance, and by approximating the trajectory as having piecewise constant acceleration that can only change its value at the end of each segment. Part deformation is taken as a nonlinear constraint which is interrelated with transfer velocity and acceleration. The relationship of deformation with transfer dynamics is generated from FEA simulation and model fitting. The developed methodology is effective when multiple static obstacles are present in the environment and the obstacles are located in complex configurations. This methodology can handle material yield constraint, material handling system capability constraint, and trajectory smoothness constraint. Simulations also show that with increase of part deflection specification, the optimal transfer time is reduced. However, the length of the geometric path is not necessarily shortened. When trajectory smoothness is increased, the geometrical deviation of the transfer path from the straight line path increases. The limitations of the developed methodology are that it does not consider part rotation during transfer process and obstacles are simplified as one dimensional objects.

The developed methodology will fill in the current absence of design guide for material handing development and simultaneously provide a mathematical tool to significantly enhance the production efficiency in manufacturing of compliant sheet metal parts.

Acknowledgement

This research was partially supported by the Atlas Technologies Inc., DaimlerChrysler, General Motors and State of Wisconsin's IEDR Program. We also would like to acknowledge Michael Austin from Atlas Technologies Inc. for earlier discussions and support.

References

[1] Li, D., Ceglarek, D., and Shi, J., 1993, ''Sliding Door Process Variation Study,'' *Technical Report*, University of Michigan, Ann Arbor.
[2] Ceglarek, D., and Shi, J., 1995, ''Dimensional Variation Reduction for Automotive Body Assembly,'' Manufacturing Review, **8**(2), pp. 139–154.
[3] Wu, X., Shi, J., and Hu, S., 1996, ''On-Site Measurement and Process Monitoring for Stamping Variation Reduction,'' *Technical Report, the 2mm Program, NIST-Advanced Technology Program*, pp. 61–80.
[4] Ceglarek, D., Li, H. F., and Tang, Y., 2001, ''Modeling and Optimization of Fixture For Handling Compliant Sheet Metal Parts,'' ASME J. Manuf. Sci. Eng., **123**(3), pp. 473–480.
[5] Li, H. F., Ceglarek, D., and Shi, J., 2002, ''A Dexterous Part Holding Model for Handling Compliant Sheet Metal Parts,'' ASME J. Manuf. Sci. Eng., **123**(1), pp. 109–118.
[6] Sprow, E., 1991, ''Sheet Metal FMS: Too Big a Jump,'' Tooling and Production, **57(7)**, pp. 53–55.
[7] Erdmann, M., and Lozano-Perez, T., 1987, ''On Multiple Moving Objects,'' Algorithmica, **2**(4), pp. 477–521.
[8] Sutner, K., and Maass, W., 1988, ''Motion Planning among Time Dependent Obstacles,'' Acta Informatica, **26**, pp. 93–122.
[9] Brady, M., Hollerbach, J., Johnson T., Lozano-Perez, T., and Mason, M., 1982, *Robot Motion: Planning and Control*. MIT Press, Cambridge.
[10] Latombe, J. C., 1991, *Robot Motion Planning*, Kluwer Academic Publishers (SECS0124), Boston/Dordrecht/London.
[11] Laumond, J.-P., 1998, *Robot Motion Planning and Control*, Springer-Verlag, London Ltd.
[12] Fujimura, K., and Samet, H., 1989, ''Hierarchical Strategy for Path Planning Among Moving Obstacles,'' IEEE Trans. Rob. Autom., **5**(1), pp. 61–69.
[13] Fraichard, T., 1999, ''Trajectory Planning in a Dynamic Workspace: a 'State-Time Space' Approach,'' Advanced Robotics, **13**(1), pp. 75–94.
[14] Constantinescu, D., and Croft, E. A., 2000, ''Smooth and Time-Optimal Trajectory Planning for Industrial Manipulators along Specified Paths,'' J. Rob. Syst., **17**(5), pp. 223–249.
[15] Kahn, M. E., and Roth, B., 1971, ''The Near-Minimum-Time Control of Open-Loop Articulated Kinematic Chains,'' ASME J. Dyn. Syst., Meas., Control, **93**, pp. 164–172.
[16] Croft, E. A., Benhabib, B., and Fenton, R. G., 1995, ''Near-Time Optimal Robot Motion Planning for On-Line Applications,'' J. Rob. Syst., **12**, pp. 553–567.
[17] Bobrow, J. E., Dubowsky, S., and Gibson, J. S., 1985, ''Time-Optimal Control of Robotic Manipulators along Specified Paths,'' Int. J. Robot. Res., **4**(3), pp. 3–17.
[18] Shiller, Z., 1994, ''On Singular Time-Optimal Control Along Specified Paths,'' IEEE J. Rob. Autom., **10**(4), pp. 561–566.
[19] Chen, Y., and Desrochers, A. A., 1990, ''A Proof of The Structure of The Minimum-Time Control Law of Robotic Manipulators Using a Hamiltonian Formulation,'' IEEE Trans. Rob. Autom., **6**(3), pp. 388–393.
[20] Chiang, A. C., 1992, *Elements of Dynamic Optimization*, McGraw-Hill Inc.
[21] Jutard-Malinge, A. D., and Bessonnet, G., 1997, ''Optimal Path Planning of Manipulatory Systems Subjected to Non-Autonomous Motion Laws,'' Robotica **15**, pp. 251–261.
[22] Shin, K. G., and McKay, N. D., 1986, ''A Dynamic Programming Approach to Trajectory Planning of Robotic Manipulators,'' IEEE Trans. Autom. Control, **AC-31**(6), pp. 491–500.
[23] Yen, C. W. V., and Liu, T. Z., 1998, ''Path Constrained Time-Optimal Trajectory Planning for X-Y Robots via an Efficient Dynamic Programming Method,'' Robotica, **16**, pp. 89–96.
[24] Zheng, Y. F., and Chen, M. Z., 1994, ''Trajectory Planning for Two Manipulators to Deform Flexible Beams,'' Robotics and Autonomous Systems, **12**(1–2), pp. 55–67.
[25] Lamiraux, F., and Kavraki, L. E., 1999, ''Path Planning for Elastic Plates Under Manipulation Constraints,'' Proc. IEEE Int. Conf. on Robotics & Automation, pp. 151–156.
[26] Chen, M. Z., and Zheng, Y. F., 1995, ''Vibration-Free Handling of Deformable Beams by Robot End-Effectors,'' J. Rob. Syst., **12**(5), pp. 331–347.
[27] Yuen, K. M., and Bone, G. M., 1996, ''Robotic Assembly of Flexible Sheet Metal Parts,'' Proc. IEEE Int. Conf. on Robotics & Automation, pp. 1511–1516.
[28] Leissa, A. W., 1969, *Vibration of Plates*, Scientific and Technical Information Division, Office of Technology Utilization, National Aeronautics and Space Administration.
[29] Roark, R. J., 1989, *Roark's Formulas for Stress and Strain*, McGraw-Hill Inc.
[30] Wu, C. F. J., Hamada, M., 2000, *Experiments: Planning, Analysis, and Parameter Design Optimization*, John Wiley and Sons.
[31] Fourer, R., Gay, D. M., and Kernighan B. W., 1993, *AMPL: A Modeling Language for Mathematical Programming*, Scientific Press.
[32] Conn, A. R., Gould, N. I. M., and Toint, Ph. L., 1992, Lancelot: A Fortran Package for Large-Scale Nonlinear Optimization (Release A), Springer-Verlag Inc.
[33] Conn, A. R., Coulman, P. K., Haring, R. A., Morril, G. L., and Visweswariach, C., 1996, ''Optimization of Custom MOS Circuits by Transistor Sizing,'' 1996 IEEE/ACM International Conference on Computer-Aided Design, IEEE 1063-6757/96, pp. 174–180.
[34] Conn, A. R., Gould, N. I. M., and Toint, Ph. L., 1996, ''Numerical Experiments with the LANCELOT Package (Release A) for Large-scale Nonlinear Optimization,'' Math. Program., **73**, pp. 73–110.